







APPLIED COMPARATIVE STUDY OF EXISTING METHODS FOR STATE-OF-CHARGE ESTIMATION IN LITHIUM-ION BATTERIES

ESTUDIO COMPARATIVO APLICADO DE MÉTODOS EXISTENTES PARA ESTIMACIÓN DEL ESTADO DE CARGA EN BATERÍAS DE IONES DE LITIO

Edwin Paccha-Herrera^{1,2,*} , Ángel Recalde^{1,3} ,
Francisco Jaramillo-Montoya⁴ , Darwin Tapia-Peralta² 

Received: 16-11-2025, Received after review: 23-03-2026, Accepted: 28-04-2026, Published: 01-07-2026

Abstract


Estimating the state of charge (SOC) of lithium-ion batteries is crucial for the operation of various electrical and electronic devices and equipment. This work presents the implementation of models based on a Bayesian approach using linearized Kalman filtering and particle filtering (PF) to estimate the SOC in lithium-ion batteries. state equation of the Bayesian models incorporates battery resistance as an artificial evolution parameter. Two models based on machine learning algorithms, random forest and K-nearest neighbors (KNN), are also implemented by fitting the parameters of an equivalent electric circuit model to electrochemical impedance spectroscopy measurements. A cylindrical LCO 26650 cell was employed in this study. The results show high performance in SOC estimation for the Bayesian filters, with PF exhibiting the best metrics, including an R^2 adjustment factor of 0.9968.


Keywords: Bayesian filtering, EIS, machine learning, SOC


Resumen


Estimar el estado de carga (SOC) de las baterías de iones de litio es crucial para la operación de diversos dispositivos y equipos eléctricos y electrónicos. Este trabajo presenta la implementación de modelos basados en un enfoque bayesiano mediante el filtro de Kalman linealizado y el filtro de partículas (PF) para estimar el SOC en baterías de iones de litio. La ecuación de estado de los modelos bayesianos incorpora la resistencia de la batería como un parámetro de evolución artificial. De igual manera, se implementan dos modelos basados en algoritmos de aprendizaje automático: random forest y KNN, mediante el ajuste de parámetros de un circuito eléctrico equivalente a las curvas de mediciones de espectroscopía de impedancia electroquímica. Se utilizó una batería cilíndrica LCO tipo 26650. Los resultados muestran un alto desempeño en la estimación del SOC para los filtros bayesianos, entre los cuales el PF presenta las mejores métricas, con un coeficiente de determinación R^2 de 0.9968.

Palabras clave: aprendizaje de máquinas, EIS, filtro bayesiano, SOC

^{1,*}Facultad de Sistemas y Telecomunicaciones, Universidad Estatal Península de Santa Elena, Ecuador. 

²Facultad de Energía, Universidad Nacional de Loja, Ecuador. 

³Facultad de Ingeniería Eléctrica e Informática, Escuela Superior Politécnica del Litoral, Ecuador. 

⁴Departamento de Ingeniería Eléctrica, Universidad de Chile, Chile. 

Corresponding author ✉: edwin.paccha@unl.edu.ec.

Suggested citation: E. Paccha-Herrera, A. Recalde, F. Jaramillo-Montoya and D. Tapia-Peralta "Applied comparative study of existing methods for state-of-charge estimation in lithium-ion batteries," *Ingenius, Revista de Ciencia y Tecnología*, N.º 36, pp. 125-136, 2026, DOI: <https://doi.org/10.17163/ings.n36.2026.10>.

1. Introduction

Lithium-ion batteries are critical components in a wide range of electrical and electronic systems, including household appliances, medical devices, laptops, electric vehicles, and energy storage systems [1]. Due to their high energy density, long lifespan, excellent efficiency, and environmentally friendly operation, Li-ion batteries have become one of the most competitive and promising energy storage technologies [2]. The state of charge (SOC) is a key parameter that provides an indirect measure of the battery's remaining usable capacity. To ensure safe and efficient operation, lithium-ion batteries rely on Battery Management Systems (BMS), which continuously monitor essential variables such as voltage, current, temperature, and capacity to estimate both the SOC and the State of Health (SOH) [3]. Monitoring these variables enables the BMS to protect the battery against overcharging, over-discharging, extreme temperatures, and overcurrents, all of which can lead to physical degradation and significantly reduce battery lifespan [4].

Several direct SOC measurement methods are available, including Coulomb counting, open-circuit voltage (OCV), electrochemical impedance spectroscopy (EIS), and internal resistance methods. In addition, indirect estimation methods predict the battery SOC using mathematical models and algorithms, generally achieving higher accuracy than direct measurement methods. Indirect estimation methods can be classified into five subgroups: model-based, adaptive filter-based, adaptive artificial intelligence-based, advanced algorithm-based, and other approaches. Model-based methods rely on algorithms that create a mathematical representation of the battery's electrical behavior and characteristics. This approach includes the electrical circuit model (ECM) and the electrochemical model (EChM), which are widely used for SOC estimation and serve as the basis for various battery modeling techniques [5].

In [6], the author proposes a model employing a polynomial algorithm-based fitting approach. This approach does not require a thermal model and provides a means of correcting temperature-induced errors. The study in [7] reports that fractional-order models can achieve higher accuracy than their integer-order counterparts, although this improvement comes at the cost of increased complexity. Moreover, physical parameters can be considered in SOC estimation. For instance, the dependence of SOC estimation on the battery's internal resistance can be exploited to obtain more accurate results [8]. Temperature effects can also cause inconsistencies in the SOC estimation of a battery pack [9].

Electrochemical Impedance Spectroscopy (EIS) is a powerful technique for battery characterization. The EIS experiment is based on the application of an alter-

nating signal across a range of frequencies. The resulting current and voltage data are correlated to identify impedances, which provide insight into electrochemical processes in the battery, such as charge transfer kinetics, ion diffusion, and interfacial reactions [10]. The EIS approach can be employed to improve SOC and SOH estimation [11]. One disadvantage of EIS is that it requires specific testing equipment and environmental temperature control to obtain more reliable results.

On the other hand, data-driven models are based on battery data, including temperature, voltage, and current measurements. These models may use simpler formulations or even operate without an explicit model, although their accuracy decreases when the input data are noisy or incomplete. However, they are more flexible because they do not require a specific battery model and demand fewer resources. The data-driven SOC estimation process comprises three key stages: data collection, model training, and SOC estimation. Some widely used techniques include Artificial Neural Networks (ANNs), Support Vector Regression (SVR), Support Vector Machines (SVMs), and Fuzzy Logic [2].

This article explores and compares different SOC estimation methods, with particular emphasis on the influence of internal resistance on SOC. The understanding and implementation of linear, nonlinear, and artificial intelligence-based models provide a new perspective for exploring the limitations of current methods and improving their robustness and adaptability under various operating conditions. Both direct and indirect models are presented. The direct approach is based on EIS measurements, where SOC is predicted using RF and KNN algorithms. The proposed indirect approaches are the linearized Kalman filter and particle filter, where a driving-cycle current profile is employed to estimate the battery SOC. By comparing different SOC estimation methods, it is possible to identify the most suitable and robust model for each operating condition, thereby improving BMS decision-making. This study paves the way for optimizing the performance and extending the lifetime of lithium-ion batteries, benefiting multiple industries and contributing to the development of more sustainable and efficient technologies.

This paper is structured as follows. The Introduction presents an overview of SOC estimation. The Materials and Methods section describes the techniques employed to estimate the SOC of the Li-ion battery under study. The Results and Discussion section presents the main findings and compares the metrics computed for each SOC estimation approach. Finally, the Conclusions section summarizes the main contributions and provides recommendations for future work.

1.1. Related work

The most common approaches applied to SOC estimation are the Coulomb counting method, also known as ampere-hour integration, the OCV method, data-driven approaches, and model-based methods [12]. The Coulomb counting method has been employed to estimate heat generation in a single Li-ion cell [13]. The authors in [14] affirm that a long short-term memory (LSTM) neural network model achieves high accuracy in estimating the SOC of a group of batteries compared with other neural network models. The LSTM-based algorithm can be improved by integrating clustering based on K-means and fuzzy C-means techniques [15]. In addition, an LSTM-based model can consider different temperatures and aging conditions to estimate SOC more accurately [16].

To address the cumulative error of the Coulomb counting method, [17] formulated an extended Kalman filter using the ampere-hour definition of SOC and a Thevenin model. This model can be improved using a nonlinear formulation based on the particle filter (PF). For instance, [18] employed a PF enhanced by an H-infinity filter to estimate SOC in an electric vehicle. Standard driving cycles were used.

Moreover, equivalent circuit models (ECMs) are commonly used with EIS measurements by combining electrical components and adjusting their parameters to minimize the discrepancy between collected data and modeled impedance spectra [19]. For example, [20] performed battery SOC estimation using an ECM based on EIS measurements combined with machine learning algorithms. Seven parameters were employed, including fractional-order elements. This approach reduces training time and is suitable for online SOC estimation.

2. Materials and methods

2.1. State of Charge definition

The SOC of a battery represents the relationship between the residual capacity Q_t and the nominal capacity Q_n and can be formulated as follows:

$$SOC(t) = \frac{Q_t}{Q_n} \times 100 \quad (1)$$

Furthermore, the SOC can be expressed as [21]:

$$SOC(t) = SOC_0 - \frac{\eta \int_{t_0}^t i(\tau) d\tau}{Q_n} \quad (2)$$

where SOC_0 is the initial value, and $I(t)$ is the real-time current, with $I(t) < 0$ for charging and $I(t) > 0$ for discharging. The parameter η denotes the Coulomb efficiency, defined as the ratio of the total charge removed from the battery to the total charge supplied during a complete cycle.

This study aims to compare direct and indirect methods for estimating the SOC in Li-ion batteries. The direct method was established based on EIS experiments. The indirect methods were based on Bayesian algorithms, namely the Kalman filter (KF) and particle filter (PF). A 26650 lithium-cobalt oxide (LCO) battery with a capacity of 4 Ah was employed.

2.2. SOC estimated based on Electrochemical impedance spectroscopy (EIS)

Results from EIS experiments are commonly presented using Nyquist diagrams, as shown in Figure 1. An ECM can be formulated for the corresponding EIS spectra. The pure ohmic resistance R_e is the value at the intersection of the curve with the horizontal axis [22]; the inductance L models the electromagnetic phenomena in the battery. The mid-frequency zone represents the charge transfer region, including the charge transfer resistance R_{ct} and double-layer capacitance C_{dl} . The R_{ct} reflects the resistance associated with lithium-ion movement between the electrode and the electrolyte [23]. Finally, the low-frequency zone represents the lithium-ion diffusion process, modeled by the constant phase element Q_{dl} , where the exponent n_{dl} varies between 0, corresponding to a resistor, and 1, corresponding to a capacitor. The ECM in Figure 1 is characterized by the impedance given by [24]:

$$Z(\omega) = R_e + \frac{1}{j\omega C_{dl}} + \left[\frac{1}{Q_{dl}(j\omega)^{-n}} + R_{ct} \right]^{-1} + j\omega L \quad (3)$$

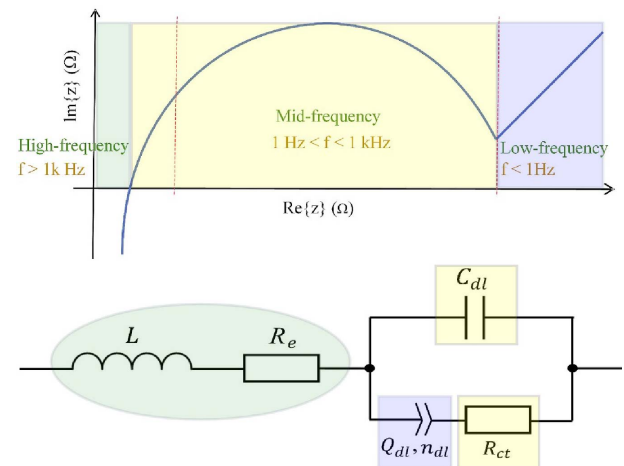


Figure 1. Nyquist plot based on EIS test of a battery and its equivalent circuit model. Adapted from [24].

In this study, SOC prediction based on EIS measurements was carried out using PGSTAT302N testing equipment. EIS was performed from 5% SOC to 100% SOC using a 4 Ah LCO 26650 Li-ion cell. A sinusoidal

current signal with an amplitude of 0.05 A was applied to the battery. Selected EIS profiles are shown in Figure 2

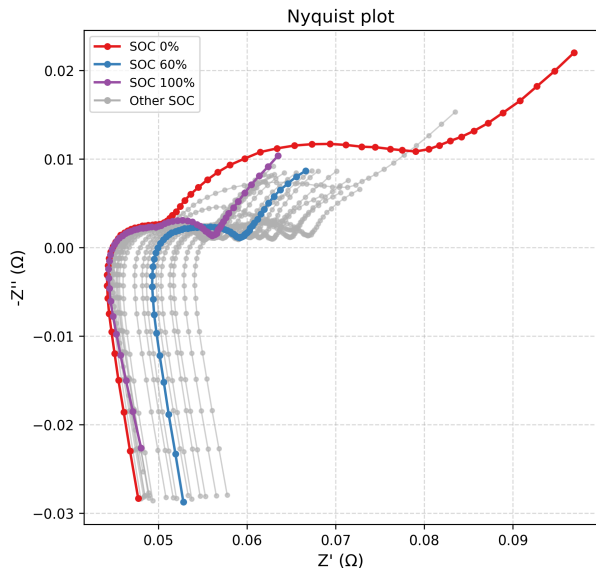


Figure 2. Nyquist plot from EIS test of the LCO 26650 battery at different SOC.

SOC estimation based on EIS measurements was performed by fitting the ECM parameters from the EIS curve and the battery terminal voltage, as illustrated in Table 1. These parameters were then used to train the RF and KNN algorithms to predict the battery SOC. Since SOC was predicted for each EIS measurement, the ECM parameters had to be fitted for each SOC measurement as well.

Table 1. Fitted parameters for the ECM at SOC 0.6.

| Parameter | Value |
|--------------------------------------|------------------------|
| C_{dl} (F) | 0.1 |
| L (H) | 5.191×10^{-7} |
| n_{dl} | 0.5 |
| Q_{dl} ($\Omega^{-1}s^{n_{dl}}$) | 1×10^{-5} |
| R_{ct} (Ω) | 0.01 |
| R_e (Ω) | 0.06662 |

RF was implemented using 100 estimators, or trees. KNN was developed using $k = 2$ nearest neighbors. In both cases, k-fold validation was performed using 5 splits and a random state of 42.

2.3. SOC estimation based on Linearized Kalman Filter

2.3.1. Linearized Kalman Filter

The Linearized Kalman Filter (LKF) is an estimation method used for nonlinear systems whose dynamics can be accurately approximated by a first-order expansion around a known reference trajectory. This

approach is widely described in the classical filtering literature [25, 26].

Consider the nonlinear system:

$$x_{k+1} = f(x_k, u_k) + w_k, \quad (4)$$

$$z_k = h(x_k) + v_k, \quad (5)$$

where x is the state-space vector, u denotes the input, z is the measurement vector, k is the time instant, w_k and v_k are zero-mean noises with covariances Q and R , respectively. The LKF assumes the existence of a nominal trajectory \bar{x}_k satisfying

$$\bar{x}_{k+1} = f(\bar{x}_k, u_k), \quad (6)$$

which represents the expected evolution in the absence of disturbances.

The error variables are defined as

$$\delta x_k = x_k - \bar{x}_k, \quad \delta z_k = z_k - h(\bar{x}_k), \quad (7)$$

and the system is linearized around \bar{x}_k using the Jacobians:

$$F_k = \left. \frac{\partial f(x, u_k)}{\partial x} \right|_{x=\bar{x}_k}, \quad (8)$$

$$H_k = \left. \frac{\partial h(x)}{\partial x} \right|_{x=\bar{x}_k}. \quad (9)$$

This yields the linear error-state model:

$$\delta x_{k+1} = F_k \delta x_k + w_k, \quad (10)$$

$$\delta z_k = H_k \delta x_k + v_k, \quad (11)$$

which defines a linear time-varying (LTV) system suitable for Kalman filtering.

The main feature of the KF is that it enables recursive estimation of a system's internal, unmeasurable states, including the SOC in the case of a battery. This is achieved by using prior knowledge, model-based predictions, and noisy measurements. The prediction and update steps are outlined below [26]:

Prediction:

$$\delta \hat{x}_{k|k-1} = F_{k-1} \delta \hat{x}_{k-1|k-1}, \quad (12)$$

$$P_{k|k-1} = F_{k-1} P_{k-1|k-1} F_{k-1}^T + Q_{k-1}. \quad (13)$$

Update:

$$K_k = P_{k|k-1} H_k^T (H_k P_{k|k-1} H_k^T + R_k)^{-1}, \quad (14)$$

$$\delta \hat{x}_{k|k} = \delta \hat{x}_{k|k-1} + K_k (\delta z_k - H_k \delta \hat{x}_{k|k-1}), \quad (15)$$

$$P_{k|k} = (I - K_k H_k) P_{k|k-1}, \quad (16)$$

where K_k is the Kalman gain matrix, P_k is the error covariance, and I is the identity matrix. The actual state estimate is then reconstructed as:

$$\hat{x}_{k|k} = \bar{x}_k + \delta \hat{x}_{k|k}. \quad (17)$$

Compared with the Extended Kalman Filter (EKF), the LKF linearizes the system only around a predefined nominal trajectory, making it suitable when this trajectory is known a priori and deviations remain small [27].

2.3.2. SOC implementation based on LKF

For this study, the state-space vector is written as:

$$x_k = \begin{bmatrix} x_{1,k} \\ x_{2,k} \end{bmatrix}, \quad (18)$$

where $x_{1,k}$ is the component associated with the internal resistance of the cell and $x_{2,k}$ is the SOC at time instant k .

The Bayesian approach requires a measurement equation. In this study, this equation corresponds to the battery voltage v_0 linearized around the point $x_0 = [x_{1,0} \ x_{2,0}]^T$ and i_0 [28]:

$$v_0 = v_L + (v_{OC} - v_L) e^{\gamma(x_{2,0}-1)} + \alpha v_L + (x_{2,0} - 1) + (1 - \alpha) v_L (e^{-\beta} - e^{-\beta \sqrt{x_{2,0}}}) - i_0 x_{1,0} \quad (19)$$

The discharging current i is the input parameter in the model, and, v_{OC} is the open-circuit voltage at 100% SOC. The parameters v_L , α , β , and γ are estimated offline and were taken from [?].

The matrices used to solve the LKF algorithm are formulated as:

$$F_k = \begin{bmatrix} 1 & 0 \\ -\frac{\Delta t}{E_{crit}} i_0 \frac{\partial v_0}{\partial x_1} & 1 - \frac{\Delta t}{E_{crit}} i_0 \frac{\partial v_0}{\partial x_2} \end{bmatrix}, \quad (20)$$

$$H_k = \begin{bmatrix} \frac{\partial v_0}{\partial x_1} & \frac{\partial v_0}{\partial x_2} \end{bmatrix}, \quad (21)$$

where E_{crit} is the critical energy, defined as the total expected energy supplied by the battery.

2.4. SOC estimation based on Particle Filter

2.4.1. Particle filter (PF)

The particle filter (PF), like the LKF, recursively estimates the *posterior* probability density function (PDF) of the unknown state vector \mathbf{x}_k , given the measurements $\mathbf{z}_{1:k}$, where $k \in \mathbb{N}$ denotes the time instant [29]. The PF represents the *posterior* PDF $p(\mathbf{x}_k | \mathbf{z}_{1:k})$ at time k using particles, defined as a set of N_p random samples with their respective weights, described in Equation (22) [30].

$$\{\mathbf{x}_k^{(i)}, w_k^{(i)}\}_{i=1}^{N_p}, \quad \sum_{i=1}^{N_p} w_k^{(i)} = 1 \quad (22)$$

To formulate the *posterior* PDF at each time instant, the PF sequentially samples the N_p particles from an alternative PDF $q(\cdot)$, known as the *importance density* [31]. Therefore, $p(\mathbf{x}_k | \mathbf{z}_{1:k})$ can be modeled as [29]:

$$p(\mathbf{x}_k | \mathbf{z}_{1:k}) \approx \sum_{i=1}^{N_p} \mathbf{w}_k^{(i)} \delta(\mathbf{x}_k - \mathbf{x}_k^{(i)}), \quad (23)$$

where the weight of each particle can be updated as follows:

$$\mathbf{w}_k^{(i)} = \mathbf{w}_{k-1}^{(i)} \frac{p(\mathbf{z}_k | \mathbf{x}_k^{(i)}) p(\mathbf{x}_k^{(i)} | \mathbf{x}_{k-1}^{(i)})}{q(\mathbf{x}_k^{(i)} | \mathbf{x}_{0:k-1}^{(i)}, \mathbf{z}_{1:k})}. \quad (24)$$

Two considerations should be taken into account. The first concerns the approximation given by Equation (23), which converges to the true *posterior* PDF $p(\mathbf{x}_k | \mathbf{z}_{1:k})$ when $N_p \rightarrow \infty$. The second concerns the design and performance of the PF implementation, which depend on the appropriate choice of the *importance density* $q(\cdot)$. For instance, in PF implementations, the following formulation is frequently proposed [32]:

$$q(\mathbf{x}_k | \mathbf{x}_{k-1}^{(i)}, \mathbf{z}_k) = p(\mathbf{x}_k | \mathbf{x}_{k-1}^{(i)}), \quad (25)$$

where $q(\cdot)$ PDF is equal to the *prior* PDF, allowing the weight vector $\mathbf{w}_k^{(i)}$ to be updated using the likelihood function, as detailed in Equation (26):

$$\mathbf{w}_k^{(i)} = \mathbf{w}_{k-1}^{(i)} p(\mathbf{z}_k | \mathbf{x}_k^{(i)}). \quad (26)$$

2.4.2. Artificial evolution for online parameter estimation

Artificial evolution is a strategy for joint state and parameter estimation within a particle filtering framework [33]. It is particularly useful when some model parameters are unknown or vary slowly over time [34]. This approach is implemented by augmenting the state vector to include the parameter vector, which is treated as an additional state variable whose evolution is described by a random-walk process [34]. Under this

formulation, the augmented process model can be expressed as follows:

$$\mathbf{x}_k = \mathbf{f}_k(\mathbf{x}_{k-1}, \boldsymbol{\theta}_{k-1}, \mathbf{u}_{k-1}, \boldsymbol{\omega}_{k-1}), \quad (27a)$$

$$\boldsymbol{\theta}_k = \boldsymbol{\theta}_{k-1} + \boldsymbol{\eta}_{k-1}. \quad (27b)$$

The variance of the random-walk process must be carefully selected, as an inappropriate choice can significantly affect the posterior PDF estimates [35]. To address this issue, the literature reports several techniques for adjusting the random-walk variance according to specific criteria. Examples include *kernel smoothing* [33] and *outer feedback correction loops* (OFCL) [36], which have been adopted in PF-based implementations relying on artificial parameter evolution.

2.4.3. SOC implementation based on PF

First, the state-transition model is defined as follows [28]:

$$x_1(k+1) = x_1(k) + \omega_1(k) \quad (28)$$

$$x_2(k+1) = x_2(k) - v(k) \cdot i(k) \cdot \Delta t \cdot E_{\text{crit}}^{-1} + \omega_2(k). \quad (29)$$

where x_1 represents the battery internal resistance, treated as an unknown parameter to be estimated, and x_2 denotes the SOC. The PF implementation considered in this study uses the following voltage measurement model:

$$\begin{aligned} v(k) = & v_L + (v_{OC} - v_L) \cdot e^{\gamma \cdot (x_2(k) - 1)} + \\ & \alpha \cdot v_L \cdot (x_2(k) - 1) + \\ & (1 - \alpha) \cdot v_L \cdot \left(e^{-\beta} - e^{-\beta \sqrt{x_2(k)}} \right) - \\ & i(k) \cdot x_1(k) + \eta(k) \end{aligned} \quad (30)$$

Process noise (ω_1 and ω_2) and measurement noise (η) are considered in the state-space formulation.

In the PF implementation, the initial conditions (x_1 and x_2), the process noise terms (ω_1 and ω_2), and the measurement noise (η), are modeled using Gaussian distributions, i.e., $x_1(0) \sim \mathcal{N}(\mu_1, \sigma_1^2)$, $x_2(0) \sim \mathcal{N}(\mu_2, \sigma_2^2)$, $\omega_1 \sim \mathcal{N}(0, \sigma_{\omega_1}^2)$, $\omega_2 \sim \mathcal{N}(0, \sigma_{\omega_2}^2)$, and $\eta \sim \mathcal{N}(0, \sigma_{\eta}^2)$. In addition, a population of $N_p = 300$ particles was used, with each particle i initially assigned a weight $W_i = 1/N_p$. The PF parameter configuration is summarized in Table 2.

Table 2. Particle filter parameter configuration.

| Parameter | Symbol | Value |
|---------------------------------------|---------------------|----------------|
| Number of particles | N_p | 300 |
| Initial internal resistance mean | μ_1 | 0, 12 Ω |
| Initial SOC mean | μ_2 | 1,00 |
| Initial internal resistance std. dev. | σ_1 | 0,005 |
| Initial SOC std. dev. | σ_2 | 0,02 |
| ω_1 std. dev. | σ_{ω_1} | 0,001 Ω |
| ω_2 std. dev. | σ_{ω_2} | 0,0001 |
| Measurement noise std. dev. | σ_{η} | 0,001 V |

2.5. Case study

To estimate the battery SOC using KF and PF, an HFWET driving cycle was employed. A scaled discharge current profile for this cycle was applied to the 26650 lithium-ion battery with LCO chemistry, as shown in Figure 3. This profile was selected because it exhibits variable behavior, whereas a constant current profile is not adequate for characterizing the battery's SOC.

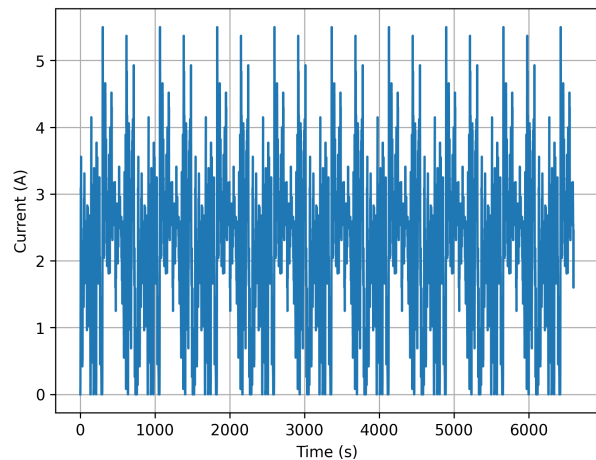


Figure 3. HFWET current profile scaled for a 4 Ah LCO battery [13].

3. Results and discussion

This section presents the results obtained from applying the SOC estimation approaches. Figures 4, 5, 6, and 7 show the SOC estimates obtained using the Kalman filter, particle filter, random forest, and KNN approaches, respectively. The last two approaches show lower fitting quality because they require more training data. Moreover, model hyperparameters could be implemented using other techniques, such as hybrid models. The PF algorithm shows robust performance due to its ability to capture nonlinear behavior and perform online estimation simultaneously. Furthermore, Bayesian algorithms are more complex to implement,

and their robustness depends on several factors, such as the process equation and the process and measurement noise terms.

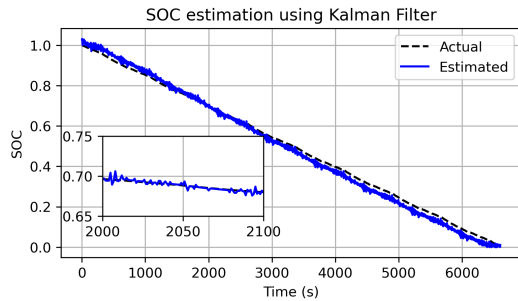


Figure 4. SOC estimation by Kalman Filter using HWFET driving profile.

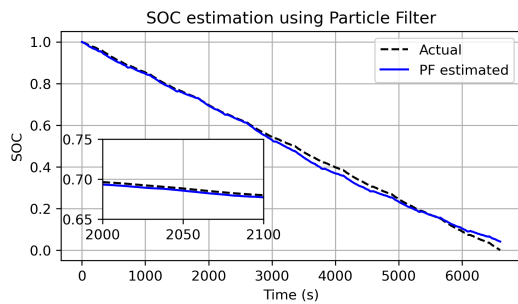


Figure 5. SOC estimation by Particle Filter using HWFET driving profile.

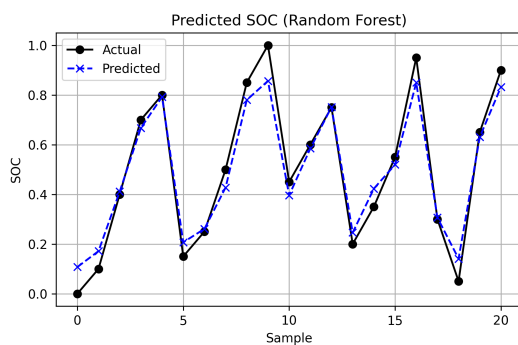


Figure 6. SOC estimation by Random Forest based on EIS.

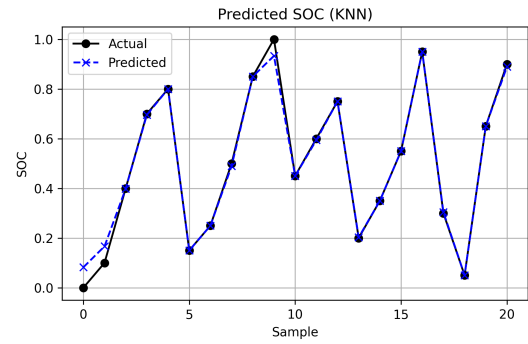


Figure 7. SOC estimation by KNN based on EIS.

Furthermore, Figure 8 and 9 show the voltage estimates obtained using the Kalman filter and particle filter, respectively. The PF provides a better fit between the real and estimated voltage.

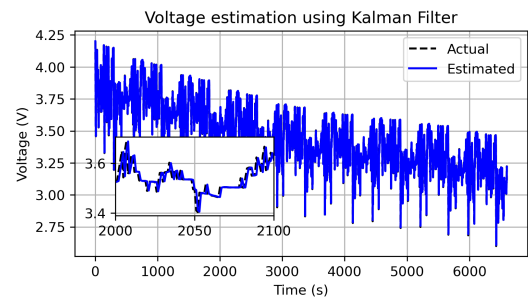


Figure 8. Voltage estimation by Kalman Filter using HWFET driving profile.

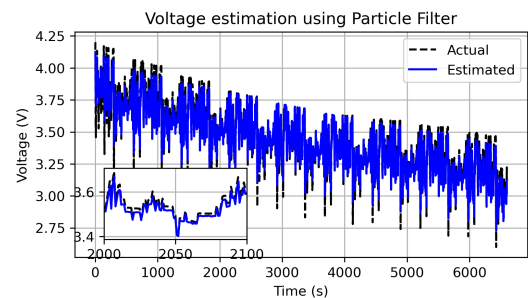


Figure 9. Voltage estimation by Particle Filter using HWFET driving profile.

One advantage of using artificial evolution for the battery resistance parameter is that its initial value is continuously adapted within the PF model, as shown in Figure 10.

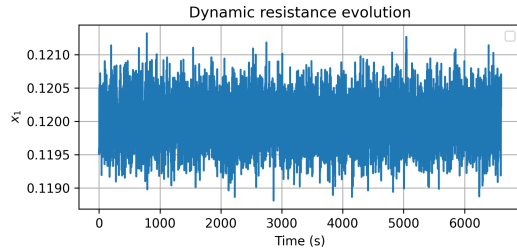


Figure 10. Artificial evolution of the battery resistance (in ohms).

A general comparison of the developed models was performed in terms of RMSE and R^2 metrics as shown in Table 3. Overall, the Bayesian approaches achieve better performance than EIS-based methods. Due to the discrete nature of EIS measurements, the RF and KNN models predict SOC only at the specific operating points where impedance spectra were acquired, rather than providing a continuous estimation over time. PF presents the best metrics due to its non-linear structure, which better captures SOC variations.

Table 3. RMSE and R^2 for SOC estimation.

| Algorithm | RMSE | R^2 |
|-----------|--------|--------|
| KF | 0.0187 | 0.9891 |
| PF | 0.0164 | 0.9968 |
| RF | 0.0644 | 0.9548 |
| KNN | 0.0276 | 0.9917 |

The comparative analysis of state-of-charge (SOC) estimation methods for lithium-ion batteries highlighted key advantages and limitations of each approach. The Kalman Filter (KF) demonstrated reliable performance in linear estimation scenarios but exhibited sensitivity to model inaccuracies and noise, which could lead to errors over extended operating periods. By contrast, the Particle Filter (PF) was robust in handling nonlinearities and uncertainties, making it particularly suitable for real-time SOC estimation in dynamic environments. However, its computational complexity remains a challenge, requiring optimized implementations for practical deployment in battery management systems (BMS). In the present approach, the PF formulation, including the process and measurement equations, and the battery parameters were adopted from [28]. That study achieved higher accuracy in SOC estimation by performing offline parameter estimation for the process equation. Another technique that could be considered to capture nonlinear behavior is the EKF, which is used in electric vehicles to provide real-time SOC estimation under different operating conditions, leading to improved BMS performance [37]. Other operating conditions and parameters that should be explored include additional driving cycles, temperature, battery aging effects, regenerative braking, and different process equations in the model.

On the other hand, machine learning-based approaches, namely RF and KNN, are less practical than Bayesian approaches. RF and KNN predict SOC using EIS measurements, but these experiments require complex equipment and are not suitable for online implementation. The results are restricted to the SOC values for which experimental EIS data are available. Moreover, machine learning algorithms require the tuning of several parameters. Similar metrics to those shown in Table 3 for RF and KNN SOC prediction were reported in [24].

The results indicate that model-based approaches, such as KF and PF, remain essential because of their maturity and real-time applicability, whereas machine learning-based techniques have potential for further refinement. Future work should explore hybrid methodologies that combine the strengths of both approaches by integrating online correction techniques with deep learning models to achieve robust and adaptive SOC estimation.

Figure 11 shows the RMSE of the SOC estimation as a function of the scale factor applied individually to each noise parameter. Each parameter was varied by multiplying its nominal value by different scale factors, while all remaining parameters were kept at their nominal configuration. The PF shows low sensitivity to σ_{ω_1} and σ_{η} , with RMSE remaining stable at approximately 0.016–0.019 across the full range evaluated. The SOC process noise σ_{ω_2} shows the highest sensitivity: values below the nominal configuration cause RMSE to exceed 0.059, as an overly constrained state transition prevents adequate particle diversity. Similarly, the likelihood kernel variance σ_v^2 degrades estimation accuracy at both extremes. Overall, the nominal configuration, corresponding to a scale factor of 1.0 with the selected parameters, yields the lowest RMSE across all parameters.

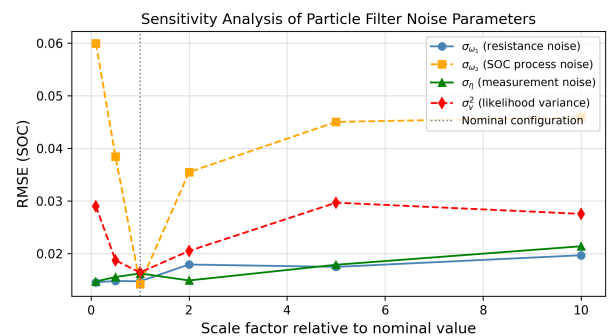


Figure 11. Sensitivity analysis of PF noise parameters.

Considering that this study is mainly applicable to battery BMS, some important aspects of this system are discussed. Table 4 presents the computational cost and embedded feasibility of the different approaches used to estimate the battery SOC. Estimators based

on the KF algorithm stand out because of their accuracy, low-to-medium memory consumption, and high feasibility for integration into embedded systems. On

the other hand, EIS-based machine learning models are not sufficiently developed for implementation in embedded systems, despite their high accuracy.

Table 4. Comparative analysis of computational cost and embedded feasibility for SOC estimation methods.

| Method | Typical Accuracy | Computational Cost | Memory Usage | Inference Time | Embedded Feasibility | Validated Platform |
|-----------------|--------------------------|--------------------|--------------|--------------------------|----------------------|------------------------------|
| LKF | High ($\leq 2\%$) | Low–Medium | Low–Medium | <1 ms | High | STM32, ARM Cortex-M [38, 39] |
| PF | Very High ($\leq 1\%$) | Very High | High | 10–100 ms (per particle) | Low | FPGA, STM32F4 [40, 41] |
| KNN (EIS-based) | High | High | Very High | Variable (dataset size) | Low | Offline only |
| RF (EIS-based) | High ($\leq 3\%$) | Medium | Medium–High | 1–10 ms | Medium | Offline only |

4. Conclusions

This study demonstrates that state-of-charge (SOC) estimation methods differ significantly in accuracy, computational implementation, and adaptability to the nonlinear battery behavior induced by the applied driving cycle. The KF approach provides reliable estimates under linear assumptions but faces challenges associated with nonlinear models and noise. Nevertheless, the KF method shows high feasibility for implementation in embedded systems for SOC prediction. The PF algorithm demonstrates robustness under dynamic conditions. By contrast, because of their dependence on specific equipment, the EIS-based machine learning algorithms applied in this study are not capable of predicting online SOC behavior.

Future research should focus on optimizing hybrid SOC estimation models that integrate traditional filtering techniques with other machine learning approaches. Additionally, efforts should be made to enhance computational efficiency for real-time applications and expand training datasets to improve the generalization capability of data-driven models. Validation under real operating conditions in electric vehicles and energy storage systems is essential to confirm the practical applicability and reliability of these estimation and prediction methods.

Contributor role

- **Edwin Paccha-Herrera:** conceptualization, methodology, software, writing – original draft.
- **Ángel Recalde:** conceptualization, formal analysis, writing – review and editing.
- **Francisco Jaramillo-Montoya:** methodology, validation, writing – review and editing.

- **Darwin Tapia-Peralta:** formal analysis, visualization, resources.

References

- [1] R. Hema and M. J. Venkatarangan, “Advancing sustainable development: Introducing a novel fast charging technique for li-ion batteries with supercapacitor integration,” *Computers and Electrical Engineering*, vol. 120, p. 109810, 2024. [Online]. Available: <https://doi.org/10.1016/j.compeleceng.2024.109810>
- [2] D. V. S. R. Sesidhar, C. Badachi, and R. C. Green II, “A review on data-driven SOC estimation with Li-ion batteries: Implementation methods & future aspirations,” *Journal of Energy Storage*, vol. 72, p. 108420, 2023. [Online]. Available: <https://doi.org/10.1016/j.est.2023.108420>
- [3] Y. Tavakol-Moghaddam, M. Boroushaki, and M. Astaneh, “Reinforcement learning for battery energy management: A new balancing approach for Li-ion battery packs,” *Results in Engineering*, vol. 23, p. 102532, 2024. [Online]. Available: <https://doi.org/10.1016/j.rineng.2024.102532>
- [4] O. Demirci, S. Taskin, E. Schaltz, and B. Acar Demirci, “Review of battery state estimation methods for electric vehicles - Part I: SOC estimation,” *Journal of Energy Storage*, vol. 87, p. 111435, 2024. [Online]. Available: <https://doi.org/10.1016/j.est.2024.111435>
- [5] Q. Wang, J. Wang, P. Zhao, J. Kang, F. Yan, and C. Du, “Correlation between the model accuracy and model-based SOC estimation,” *Electrochimica Acta*, vol. 228, pp. 146–159, 2017. [Online]. Available: <https://doi.org/10.1016/j.electacta.2017.01.057>

- [6] A. Tabine, E. M. Laadissi, H. Mastouri, A. Elachhab, S. Bouzaid, and A. Hajjaji, "A novel fitting polynomial approach for an accurate SOC estimation in Li-ion batteries in view of temperature variations," *Results in Engineering*, p. 103962, 2025. [Online]. Available: <https://doi.org/10.1016/j.rineng.2025.103962>
- [7] C. Zou, L. Zhang, X. Hu, Z. Wang, T. Wik, and M. Pecht, "A review of fractional-order techniques applied to lithium-ion batteries, lead-acid batteries, and supercapacitors," *Journal of Power Sources*, vol. 390, pp. 286–296, 2018. [Online]. Available: <https://doi.org/10.1016/j.jpowsour.2018.04.033>
- [8] C. Xu, T. Cleary, and H. K. Fathy, "Improving Li-S battery SOC estimation using an SOC-dependent resistance model," *IFAC-PapersOnLine*, vol. 56, no. 3, pp. 439–444, 2023, 3rd Modeling, Estimation and Control Conference MECC 2023. [Online]. Available: <https://doi.org/10.1016/j.ifacol.2023.12.063>
- [9] H. Ren, L. Jia, L. Yin, C. Dang, and Z. Chen, "Research on battery pack SOC consistency based on the electric-thermal-fluid coupling model," *Journal of Energy Storage*, vol. 97, p. 112924, 2024. [Online]. Available: <https://doi.org/10.1016/j.est.2024.112924>
- [10] A. C. Lazanas and M. I. Prodromidis, "Electrochemical impedance spectroscopy—A tutorial," *ACS Measurement Science Au*, vol. 3, no. 3, pp. 162–193, 2023. [Online]. Available: <https://doi.org/10.1021/acsmeasuresciau.2c00070>
- [11] H. Mustafa, C. Bourelly, M. Vitelli, F. Milano, M. Molinara, and L. Ferrigno, "SOC estimation on Li-ion batteries: A new EIS-based dataset for data-driven applications," *Data in Brief*, vol. 57, p. 110947, 2024. [Online]. Available: <https://doi.org/10.1016/j.dib.2024.110947>
- [12] C. Wang, M. Yang, X. Wang, Z. Xiong, F. Qian, C. Deng, C. Yu, Z. Zhang, and X. Guo, "A review of battery SOC estimation based on equivalent circuit models," *Journal of Energy Storage*, vol. 110, p. 115346, 2025. [Online]. Available: <https://doi.org/10.1016/j.est.2025.115346>
- [13] E. Paccha-Herrera, W. R. Calderón-Muñoz, M. Orchard, F. Jaramillo, and K. Medjaher, "Thermal modeling approaches for a LiCoO₂ lithium-ion battery—A comparative study with experimental validation," *Batteries*, vol. 6, no. 3, 2020. [Online]. Available: <https://doi.org/10.3390/batteries6030040>
- [14] E. Almaita, S. Alshkoor, E. Abdelsalam, and F. Almomani, "State of charge estimation for a group of lithium-ion batteries using long short-term memory neural network," *Journal of Energy Storage*, vol. 52, p. 104761, 2022. [Online]. Available: <https://doi.org/10.1016/j.est.2022.104761>
- [15] M. K. Al-Alawi, A. Jaddoa, J. Cugley, and H. Hassanin, "A novel enhanced SOC estimation method for lithium-ion battery cells using cluster-based LSTM models and centroid proximity selection," *Journal of Energy Storage*, vol. 97, p. 112866, 2024. [Online]. Available: <https://doi.org/10.1016/j.est.2024.112866>
- [16] G. Chen, W. Peng, and F. Yang, "An LSTM-SA model for SOC estimation of lithium-ion batteries under various temperatures and aging levels," *Journal of Energy Storage*, vol. 84, p. 110906, 2024. [Online]. Available: <https://doi.org/10.1016/j.est.2024.110906>
- [17] Z. Cui, W. Hu, G. Zhang, Z. Zhang, and Z. Chen, "An extended Kalman filter based SOC estimation method for Li-ion battery," *Energy Reports*, vol. 8, pp. 81–87, 2022, iCPE 2021 - The 2nd International Conference on Power Engineering. [Online]. Available: <https://doi.org/10.1016/j.egy.2022.02.116>
- [18] Y. Chen, R. Li, Z. Sun, L. Zhao, and X. Guo, "SOC estimation of retired lithium-ion batteries for electric vehicle with improved particle filter by H-infinity filter," *Energy Reports*, vol. 9, pp. 1937–1947, 2023. [Online]. Available: <https://doi.org/10.1016/j.egy.2023.01.018>
- [19] N. Meddings, M. Heinrich, F. Overney, J.-S. Lee, V. Ruiz, E. Napolitano, S. Seitz, G. Hinds, R. Raccichini, M. Gaberšček, and J. Park, "Application of electrochemical impedance spectroscopy to commercial Li-ion cells: A review," *Journal of Power Sources*, vol. 480, p. 228742, 2020. [Online]. Available: <https://doi.org/10.1016/j.jpowsour.2020.228742>
- [20] E. Buchicchio, A. De Angelis, F. Santoni, P. Carbone, F. Bianconi, and F. Smeraldi, "Battery SOC estimation from EIS data based on machine learning and equivalent circuit model," *Energy*, vol. 283, p. 128461, 2023. [Online]. Available: <https://doi.org/10.1016/j.energy.2023.128461>
- [21] Y. Miao and Z. Gao, "Estimation for state of charge of lithium-ion batteries by adaptive fractional-order unscented Kalman filters," *Journal of Energy Storage*, vol. 51, p. 104396, 2022. [Online]. Available: <https://doi.org/10.1016/j.est.2022.104396>

- [22] A. Barai, K. Uddin, W. D. Widanage, A. McGordon, and P. Jennings, "A study of the influence of measurement timescale on internal resistance characterisation methodologies for lithium-ion cells," *Scientific Reports*, vol. 8, no. 1, pp. 1–13, 2018. [Online]. Available: <https://doi.org/10.1038/s41598-017-18424-5>
- [23] H. Thomas and M. H. Weatherspoon, "Capacity and state-of-health prediction of lithium-ion batteries using reduced equivalent circuit models," *Batteries*, vol. 11, no. 4, 2025. [Online]. Available: <https://doi.org/10.3390/batteries11040162>
- [24] X. Zhang, L. Zhang, J. Wu, W. Bai, H. Dai, H. Lin, F. Zhang, and Y. Yang, "SOC estimation of lithium-ion batteries using equivalent circuit model and Nyquist plots from EIS data: A machine learning approach," *Journal of Electroanalytical Chemistry*, vol. 987, p. 119093, 2025. [Online]. Available: <https://doi.org/10.1016/j.jelechem.2025.119093>
- [25] D. Simon, *Optimal State Estimation: Kalman, H-Infinity, and Nonlinear Approaches*. John Wiley & Sons, 2006. [Online]. Available: <http://doi.org/10.1002/0470045345>
- [26] P. Zarchan and H. Musoff, *Fundamentals of Kalman Filtering: A Practical Approach*, 4th ed. American Institute of Aeronautics and Astronautics, Inc., 2015. [Online]. Available: <https://doi.org/10.2514/4.102776>
- [27] M. S. Grewal and A. P. Andrews, *Kalman Filtering: Theory and Practice Using MATLAB*, 3rd ed. John Wiley & Sons, 2008. [Online]. Available: <https://doi.org/10.1002/9780470377819>
- [28] D. Pola, H. Navarrete, M. Orchard, R. Rabie, M. Cerda, B. Olivares, J. Silva, P. Espinoza, and A. Perez, "Particle-filtering-based discharge time prognosis for lithium-ion batteries with a statistical characterization of use profiles," *IEEE Transactions on Reliability*, vol. 64, pp. 1–11, 2015. [Online]. Available: <https://doi.org/10.1109/TR.2014.2385069>
- [29] M. S. Arulampalam, S. Maskell, N. Gordon, and T. Clapp, "A tutorial on particle filters for online nonlinear/non-Gaussian Bayesian tracking," *IEEE Trans. Signal Process.*, vol. 50, no. 2, pp. 174–188, 2002. [Online]. Available: <https://doi.org/10.1109/78.978374>
- [30] C. Díaz, V. Quintero, A. Pérez, F. Jaramillo, C. Burgos-Mellado, H. Rozas, M. E. Orchard, D. Sáez, and R. Cárdenas, "Particle-filtering-based prognostics for the state of maximum power available in lithium-ion batteries at electromobility applications," *IEEE Trans. Veh. Technol.*, vol. 69, no. 7, pp. 7187–7200, 2020. [Online]. Available: <https://doi.org/10.1109/TVT.2020.2993949>
- [31] M. Zajac, "Online fault detection of a mobile robot with a parallelized particle filter," *Neurocomputing.*, vol. 126, pp. 151–165, 2014. [Online]. Available: <https://doi.org/10.1016/j.neucom.2012.11.049>
- [32] M. Sami Fadali, *Introduction to random signals, estimation theory, and Kalman filtering*, 1st ed. Springer Singapore, 2024. [Online]. Available: <https://doi.org/10.1007/978-981-99-8063-5>
- [33] A. Tulsyan, B. Huang, R. Bhushan Gopaluni, and J. Fraser Forbes, "On simultaneous on-line state and parameter estimation in non-linear state-space models," *J. Process Control.*, vol. 23, no. 4, pp. 516–526, 2013. [Online]. Available: <https://doi.org/10.1016/j.jprocont.2013.01.010>
- [34] Z. Hong, L. Xu, and J. Chen, "Artificial evolution based cost-reference particle filter for nonlinear state and parameter estimation in process systems with unknown noise statistics and model parameters," *J. Taiwan Inst. Chem. Eng.*, vol. 112, pp. 377–387, 2020. [Online]. Available: <https://doi.org/10.1016/j.jtice.2020.04.009>
- [35] Y. Hu, P. Baraldi, F. Di Maio, and E. Zio, "Online performance assessment method for a model-based prognostic approach," *IEEE Trans. Reliab.*, vol. 65, no. 2, pp. 718–735, 2016. [Online]. Available: <https://doi.org/10.1109/TR.2015.2500681>
- [36] M. E. Orchard, F. A. Tobar, and G. J. Vachtsevanos, "Outer Feedback Correction Loops in Particle Filtering-based Prognostic Algorithms: Statistical Performance Comparison," *Stud. Informatics Control.*, vol. 18, no. 4, pp. 295–304, 2009. [Online]. Available: <https://upsalesiana.ec/ing36ar10r36>
- [37] M. O. Oloyede, G. A. Akpakwu, H. C. Myburgh, A. De Freitas, and T. Kunatsa, "A review on state-of-charge estimation methods, energy storage technologies and state-of-the-art simulators: Recent developments and challenges," *World Electric Vehicle Journal*, vol. 15, no. 9, 2024. [Online]. Available: <https://doi.org/10.3390/wevj15090381>
- [38] A. Valade, P. Acco, P. Grabolosa, and J.-Y. Fourniols, "A study about kalman filters applied to embedded sensors," *Sensors*, vol. 17, no. 12, 2017. [Online]. Available: <https://doi.org/10.3390/s17122810>

- [39] G. Nishanth, M. M. Krishnan, B. Parandhaman, and J. Harinarayanan, “Hardware implementation of EKF based SOC estimate for lithium-ion batteries in electric vehicle applications,” *Scientific Reports*, vol. 15, no. 1, p. 15551, 2025. [Online]. Available: <https://doi.org/10.1038/s41598-025-99931-8>
- [40] J. Michalski, M. Retinger, P. Koziarski, and J. Zietkiewicz, “Temperature control unit—modeling and implementation of a particle filter on a microcontroller,” *Applied Sciences*, vol. 12, no. 15, 2022. [Online]. Available: <https://doi.org/10.3390/app12157631>
- [41] J. Schönefeld and D. Möller, “Mathematical aspects of the implementation of particle filters on FPGA,” *IFAC Proceedings Volumes*, vol. 45, no. 2, pp. 1243–1248, 2012, 7th Vienna International Conference on Mathematical Modelling. [Online]. Available: <https://doi.org/10.3182/20120215-3-AT-3016.00220>